Pancharatnam phase: A tool for atom optics

B. Décamps, A. Gauguet, J. Vigué, and M. Büchner*
Laboratoire Collisions Agrégats Réactivité-IRSAMC, Université de Toulouse-UPS and CNRS UMR 5589
118, Route de Narbonne, F-31062, Toulouse Cedex, France
(Received 14 February 2017; published 24 July 2017)

The Pancharatnam phase belongs to the family of geometric Berry phases. We use this optical phase to control the phase of our atom interferometer, which involves diffraction of the atom wave by laser standing waves in the Bragg regime. The Pancharatnam phase of the reflected beam of one standing wave controls the phase imprinted on the atom wave by the diffraction process. In addition to the expected phase shift, the experimental data exhibits the signature of several defects which are described and quantified. From this analysis, we estimate that a Pancharatnam phase shifter can be reliably used to control the phase of an atom interferometer in the sub-mrad regime. Moreover, as the geometric nature of the Pancharatnam phase renders this phase achromatic, its use in multispecies atom interferometers may be of great interest.

DOI: 10.1103/PhysRevA.96.013624

I. INTRODUCTION

Atom interferometry has been rapidly developing since 1991 and a large fraction of the impressive results thus achieved are described in a review article by Cronin *et al.* [1] and more recently in the Atom interferometry book [2] published in 2014. In this paper, we use the Pancharatnam phase of a light beam [3] to control the phase of an atom interferometer. Let us first recall what the Pancharatnam phase is before explaining its transfer to atom waves.

Following Pancharatnam and because of its tutorial interest, we have chosen to use the Poincaré sphere [4,5] rather than the Jones formalism [6] to represent the polarization state of a fully polarized light beam (see Appendix A for details).

If the representative point follows a closed path on this sphere because of its propagation through birefringent plates, this path results in a phase shift equal to $\pm\Omega/2$, where Ω is the solid angle spanned by the path on this sphere. This phase, discovered by Pancharatnam in 1956 [3], is a precursor of the geometric phase [7] discovered by Berry in 1984 (the connection between these two phases is discussed in [8]). Numerous works on the Pancharatnam phase are reviewed by Bhandari [9]. Because of its geometric nature, the Pancharatnam phase is independent of the light wavelength, a property already applied in optical interferometry for astronomy [10].

Diffraction by laser beams is the main tool for the coherent manipulation of atom waves [1]: The absorption and stimulated emission of photons transfer photon momenta to the atom and, at the same time, imprint the phase of the laser waves on the atom wave [11]. It is thus possible to imprint the Pancharatnam phase of a laser beam on an atom wave. In the present paper, we describe an experiment which uses the Pancharatnam phase to scan the fringes of our lithium atom interferometer.

The interest of using the Pancharatnam phase to control the phase of atom interferometer is twofold: (a) This phase can be controlled by rotating a quarter-wave plate and rotations can be measured with very high accuracy and (b) the achromatic character of this phase opens up the possibility of producing the same phase shift in a double atom interferometer operated simultaneously with two different atoms; such a double interferometer can be used to develop a quantum test of the Weak Equivalence Principle. After a first experimental test [12] done with ^{87}Rb-^{85}Rb, several such tests have already been performed with the K-Rb [13–15] or Yb-Rb [16] pairs and several other tests are under development [17]. In such an experiment, the measurement of the relative phase is usually done by the ellipse fitting technique [15,18,19] and, in order to minimize the relative phase extraction bias [20–22], it is important to homogeneously scan the phases for the two atomic species and such a common scan is possible thanks to the Pancharatnam phase.

Another elegant technique which permits one to scan independently two coaxial laser standing waves has been recently developed, using polarization synthesis [23] with a relative phase noise $\sim$1 mrad. This technique can compete with the use of the Pancharatnam phase for double atom interferometers, when extended to two different laser wavelengths.

The content of this article is organized as follows: We first describe how to use the Pancharatnam phase to control the phase of an atom interferometer and why it is interesting; we then discuss a simple experiment producing such a phase; we describe our experiment and its results; we analyze the defects of the system producing the Pancharatnam phase; and we discuss the prospects opened by the present study.

II. THE PANCHARATNAM AND THE ATOM INTERFEROMETER PHASES

Among the numerous processes of atom diffraction by laser [11], only the Bragg and Raman diffraction are frequently used. Bragg diffraction results from the interaction of the atom wave with a quasiresonant laser standing wave. Diffraction of order p is due to p cycles of photon absorption and stimulated emission. Because the absorbed and emitted photons have the same frequency and polarization, the diffracted atom remains in its initial internal state but its momentum has changed by $2p\hbar\mathbf{k}_L$, where $\mathbf{k}_L$ is the laser wave vector. This process occurs if the Bragg condition of order p is fulfilled and the diffraction amplitude α_p can be tuned by the choice of the laser power density, frequency detuning with respect to the atom resonance transition, and atom-laser interaction time. If the incident atom

*matthias.buchner@irsamc.ups-tlse.fr

is described by a plane wave $\psi_{\rm inc} = \exp[i\mathbf{k}\cdot\mathbf{r}]$, the diffracted wave ψ_p is given by

$$\psi_p(\mathbf{r}) \approx \alpha_p \exp[i\mathbf{k}\cdot\mathbf{r} + 2ip\mathbf{k}_L\cdot(\mathbf{r}-\mathbf{r}_0)], \quad (1)$$

where $\mathbf{r}_0$ is the position of a node of the laser standing wave (for instance, the mirror surface in the approximation of a perfect metallic mirror). Because the standing wave is produced by reflecting a laser beam, one cannot change the phase of the diffraction amplitudes α_p by modifying the laser phase (while this is possible with Raman diffraction by changing the relative phase of the two laser beams). As a consequence, with Bragg diffraction, the only way to control the phase of the diffracted atom wave is to change the positions of the nodes of the laser standing wave, for instance, by moving the mirror forming the laser standing wave. This displacement is usually done by a piezoelectric device with an excellent sensitivity in the nanometer range. Unfortunately it suffers from the well-known defects of such devices: nonlinearity, hysteresis, tilt, and creep. These defects, which limit the accuracy of the mirror displacement, can be corrected by using servo-loops coupled to a position-measuring device. Here, we replace this mirror displacement by the use of the Pancharatnam phase, which has the interest of being independent of the wavelength while the phase induced by a mirror displacement is inversely proportional to the wavelength.

A. Creation of a Pancharatnam phase

To produce a Pancharatnam phase, one of the simplest arrangement, made of two quarter-wave plates and a mirror, was described by Chyba *et al.* [24] (see also [25–27]). The phase was then measured by a Michelson interferometer, in very good agreement with theory. Figure 1 presents a schematic drawing of this setup and the circuit followed on the Poincaré sphere. In our experiment, we use the same arrangement on a laser standing wave of our atom interferometer.

B. Our atom interferometer and the Pancharatnam phase setup

Our Mach-Zehnder atom interferometer [28–30] (represented schematically in Fig. 2), is operated with a lithium atomic beam produced by a supersonic expansion of an argon-lithium mixture, with a mean lithium velocity ≈1065 m/s corresponding to a de Broglie wavelength $\lambda_{\rm dB} \approx 54$ pm. Laser diffraction in the Bragg regime is used to split, reflect, and recombine the ^{7}Li atom wave: The lithium atoms cross three quasi-resonant laser standing waves produced by reflecting three laser beams on three mirrors Mi ($i \in \{1,2,3\}$). One of the complementary output beams is selected by the detection slit DS and detected by a Langmuir-Taylor ionization detector. The detector background signal is measured by flagging the lithium beam and subtracted from the interferometer signal. The intensity $\mathcal{I}$ of the detected beam is the corrected interferometer signal given by

$$\mathcal{I} = \mathcal{I}_0[1 + \mathcal{V}\cos(\varphi_d)], \quad (2)$$

$$\text{with } \varphi_d = 2k_L(x_1 - 2x_2 + x_3), \quad (3)$$

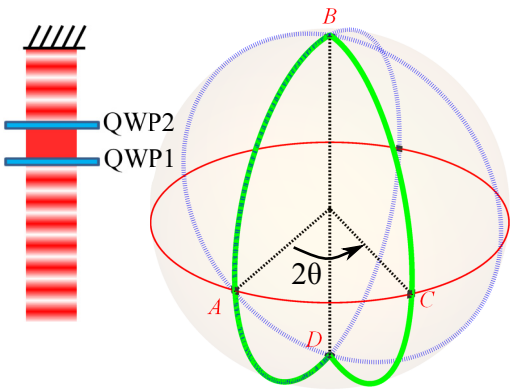

FIG. 1. (Left part) The optical arrangement of Chyba *et al.* [24]. A linearly polarized laser beam crosses two quarter-wave plates QWP1 and QWP2 before being reflected by a mirror and crossing back QWP2 and QWP1. The optical axis of QWP1 makes an angle $\pi/4$ with the polarization vector while the optical axis of QWP2 makes an angle θ with the optical axis of QWP1. (Right part) Circuit followed on the Poincaré sphere by the light beam polarization. The initial linear polarization (point A) becomes right circular after QWP1 (pole B) then linear after QWP2 (point C). The polarization, not modified by reflection on the mirror, becomes left circular after QWP2 (pole D) and back linear after QWP1 (point A). The angle between the planes BAD and BCD being equal to 2θ, the solid angle spanned by the ABCDA circuit is 4θ and the Pancharatnam phase is equal to 2θ.

where $\mathcal{I}_0$ is the mean intensity and $\mathcal{V}$ the fringe visibility. Following Eq. (1), the fringe phase φ_d is a function of x_i ($i \in \{1,2,3\}$) which is the x position of a node of the standing wave produced by mirror Mi. Usually, we scan the phase φ_d by displacing the mirror $M3$ with a piezo-electric device. For the present experiment, we use the Pancharatnam phase $\varphi_P(\theta)$ produced by a setup similar to the one of Chyba *et al.* [24], with two quarter-wave plates QWP1 and QWP2 and the mirror $M3$. QWP1 is fixed while QWP2 rotates in its plane and a rotation of QWP2 by an angle θ induces a variation $\varphi_P(\theta) = 2\theta$ of φ_d.

We have used high quality quarter-wave plates QWP1 and QWP2 made of quartz, with the following specifications:

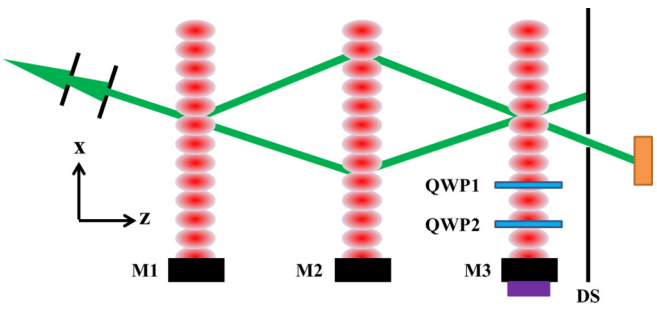

FIG. 2. Schematic drawing of our atom interferometer. A lithium atomic beam (full green lines) is diffracted by three laser standing waves produced by reflecting three laser beams on the mirrors $M1$, $M2$, and $M3$. The (violet) box below $M3$ represents the piezo-electric device which displaces this mirror in the **x** direction and modifies the diffraction phase φ_d given by Eq. (3). In the present experiment, this displacement is replaced by the Pancharatnam phase produced by the quarter-wave plates QWP1 and QWP2.

phase retardation $\pi/2 \pm \pi/150$ for the $\lambda = 671$ nm wavelength; quality of the transmitted wavefront better than $\lambda/10$; antireflection coating, with a residual reflection coefficient below 0.2% per face [31]. The ensemble made of QWP1 and QWP2 was placed between the mirror $M3$ and the arms of the atom interferometer. QWP2 was mounted on a rotatory stage, fitted with an optical encoder (Mercury 6000V encoder from MicroE) which measures the rotation angle θ with an uncertainty close to 1 mrad. The challenge was to introduce this ensemble inside the interferometer vacuum chamber, in the 30-mm space available between the rail supporting the mirrors Mi and the atom interferometer arms [32]. Because of this space limitation, it was challenging to adjust finely the QWP planes.

The interferometer signal is very sensitive to the magnetic field gradient [33,34] and it was necessary to build the support of QW1 and QWP2 with nonferromagnetic components: We used a plastic ball bearing with glass balls for the rotatory stage. The rotation was transmitted by a plastic worm drive from a synchronous electric motor located outside the vacuum chamber, at ∼25 cm above the atom interferometer plane.

Before putting this ensemble under vacuum, we aligned the QWP2 plane to be as perpendicular as possible to its rotation axis and QWP1 to be as parallel as possible to the mean plane of QWP2. Then, with the ensemble in place, these two planes were adjusted to be as parallel as possible to the laser standing wave mirror $M3$. The angle between the optical axis of QWP1 and the polarization vector of the incident laser beam was then adjusted to $\pi/4$ with an uncertainty ϵ_p smaller than 30 mrad. Finally, as shown by Eq. (3), any motion of the mirrors Mi modifies the phase of the interference signals and, in order to minimize these motions, the ensemble made of QWP1 and QWP2 was suspended from the top of the vacuum chamber. A consequence of this choice is that the altitudes of the rotation axis of QWP2 and of the atom interferometer arms may differ by ∼1 mm.

III. RESULTS

With the atom interferometer in operation, we have first optimized the atom interference fringe signal and we have then used the Pancharatnam phase to record the fringes presented in Fig. 3: The fitted visibility $\mathcal{V} = 0.743(16)$ is identical to the one observed when we displace the mirror $M3$.

The inhomogeneities of the quarter-wave plates distort the laser standing wave and these distortions produce a phase spread on the diffracted atom wave and a reduction of the fringe visibility. The observed value of this visibility, not substantially lower than the one routinely obtained with our interferometer, proves that these distortions are small. When using a Pancharatnam phase, it is possible to scan indefinitely in the same direction, whereas this is not possible by displacing $M3$, but the recorded fringes are not exactly sinusoidal contrarily to the theoretical predictions. Indeed several defects of our optical arrangement explain this deviation. Here are, for each defect, its origin and its contribution to φ_d (the detailed calculations are given in the appendixes).

(a) The rotating quarter-wave plate QWP2 is slightly prismatic, with a wedge angle $\alpha \approx 10$ μrad (this angle, which is usually not specified in quarter-wave plates, can be substantially reduced). If δr is the distance between the center of rotation of QWP2 and the center of the laser beam's part sampled by the atoms, the rotation of QWP2 produces a modulation of the optical path which results in a phase shift $\varphi_{\mathrm{dyn},1}$:

$$\varphi_{\mathrm{dyn},1} = 2k_L(\bar{n} - 1)\delta r\alpha \cos(\theta - C_1), \tag{4}$$

where $\bar{n} = 1.547$ is the mean refractive index of quartz. For $\delta r \approx 1$ mm, the amplitude $\phi_{\mathrm{dyn},1}$ is ≈0.1 rad.

(b) The rotation axis **R** of QWP2, the normal **N** to its face, and the laser beam axis **L** are not exactly parallel. If β is the angle between **N** and **L** and if γ is the angle between **R** and **L**, the rotation of QWP2 modulates the optical path which results in a phase shift $\varphi_{\mathrm{dyn},2}$:

$$\varphi_{\mathrm{dyn},2} \approx 2k_L\bar{e}\frac{\bar{n} - 1}{\bar{n}}\beta\gamma \cos(\theta - C_2), \tag{5}$$

where $\bar{e} \sim 1$ mm is the mean thickness of QWP2. We estimate that the $\beta\gamma$ product should not exceed 5×10^{-5} rad^2 and for this value, we find $\varphi_{\mathrm{dyn},2} \approx 0.3$ rad. $\varphi_{\mathrm{dyn},1}$ and $\varphi_{\mathrm{dyn},2}$ have the same period equal to a full rotation of QWP2.

(c) If the phase retardation of QWP1 and QWP2 differ from their design value $\pi/2$, the path on the Poincaré sphere and the Pancharatnam phase are both modified. We note $\pi/2 + \varepsilon_I$ the retardation of QWP$_I$ ($I = 1,2$), with $\varepsilon_I \ll 1$. The modified Pancharatnam phase $\varphi_{P,1}$ is given by

$$\varphi_{P,1}(\theta) \approx \varphi_P(\theta) + 2(\varepsilon_1 + \varepsilon_2)\sin(2\theta) - \varepsilon_1 \sin(4\theta) + \tfrac{3}{4}\left[4\varepsilon_1\varepsilon_2 \sin(2\theta) - \varepsilon_1^2 \sin(4\theta)\right], \tag{6}$$

up to second-order terms in ε_I. In addition to the ideal Pancharatnam phase $\varphi_P(\theta) = 2\theta$, we get corrections which are sinusoidal functions of 2θ and 4θ. From the plate specification $|\varepsilon_I| < 2 \times 10^{-2}$ rad, we find that the first-order term is smaller than 9×10^{-2} rad and the second-order term is smaller than 2×10^{-3} rad.

(d) The angle between incident polarization and the axes of QWP1 may differ from $\pi/4$. If this angle is equal to $\pi/4 + \epsilon_p$,

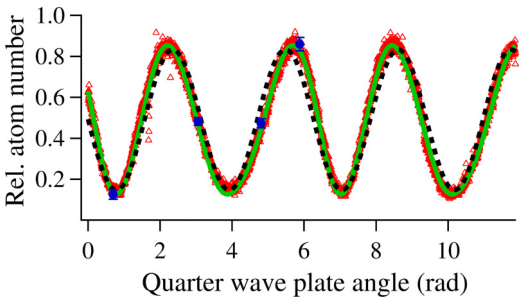

FIG. 3. Atom interference fringes obtained by the rotation of QWP2. The (red) triangles correspond to the atom count each 100 ms, normalized to the atom flux [i.e., $\mathcal{I}/(2\mathcal{I}_0)$]. Four (blue) circles indicate typical error bars. The (black) dotted line results from a fit assuming an ideal Pancharatnam phase $\varphi_d = 2(\theta - \theta_0)$: There are systematic deviations due to the defects described by Eq. (8). The (green) solid line results from a second fit using Eq. (8) with the following fitted values $u_1 = 0.38(3)$ rad, $u_2 = 0.03(1)$ rad, and $u_3 = 0.000(2)$ rad (see text).

the Pancharatnam phase $\phi_{P,2}$ becomes

$$\varphi_{P,2}(\theta) \approx \varphi_P(\theta) + 2\epsilon_p[2\cos(2\theta) - 1 - \cos(4\theta)] - \epsilon_p^2 \sin(4\theta), \quad (7)$$

up to second order in ϵ_p. The correction linear in ϵ_p contains sinusoidal functions of 2θ and 4θ, with an amplitude equal to 0.06 rad if ϵ_p reaches its maximum value 30 mrad, while the second-order term accounts for less than 10^{-3} rad.

In summary, $\varphi_{\mathrm{dyn},1}$ and $\varphi_{\mathrm{dyn},2}$ are the dominant corrections, with magnitudes 0.1–0.3 rad and the same period equal to a full turn of QWP2. They can be represented by a single sinusoidal function of θ. The modifications of the Pancharatnam phase due to the QWP retardation or to misalignment of the incident polarization have smaller amplitudes of the order of 0.1 rad and they have a period equal to half a turn of QWP2. Summarizing the different contributions, the phase φ_d is given by

$$\begin{aligned}\varphi_d = {} & 2(\theta - \theta_0) + u_1 \sin(\theta - \theta_1) \\ & + u_2\{2\cos[2(\theta - \theta_0)] - 2\cos^2[2(\theta - \theta_0)]\} \\ & + u_3\{4\sin[2(\theta - \theta_0)] - \sin[4(\theta - \theta_0)]\}, \end{aligned} \quad (8)$$

where we have kept only the lowest order terms and have assumed, for simplicity, that the two QWP have identical ε_I. The constant θ_0 takes into account that our measurement of QWP2's rotation angle θ is made with an arbitrary origin and for the optical path dependent terms, we must use a different phase reference θ_1 as the geometrical orientation is independent of the optical axis orientation. We have used this equation to fit the measured fringes and the best fit of our experimental data represented in Fig. 3 is quite good. Indeed, the dynamical terms amplitude [$u_1 = 0.38(3)$ rad] is coherent with our estimated values, 0.1 and 0.3, whose sum depends on the relative differential phases C_1 and C_2 of Eqs. (4) and (5) which were not measured. The two other parameters $u_2 = 0.03(1)$ rad and $u_3 = 0.000(2)$ rad are compatible with our conservative estimates 0.06 and 0.02, respectively.

IV. CONCLUSION

In this paper we have demonstrated the use of the Pancharatnam phase for the control of an atom interferometer's phase. However, in addition to the ideal Pancharatnam phase, we have observed supplementary phase shifts due to experimental defects.

The dominant defects are presently due to the prismatic shape of the rotating quarter-wave plate and to a misalignment effect. As discussed in Appendix C, these two effects can be reduced below 10^{-3} rad, where they should be negligible for most experiments.

The defects of the Pancharatnam phase itself are due to incorrect values of the retardation of QWP1 and QWP2 and to an incorrect direction of the incident polarization with respect to QWP1 axes. These defects were barely accessible in our experiment but they represent the fundamental limitations of the technique. The retardation of a phase plate can be measured with an uncertainty smaller than 10^{-3} rad [35–37] or even 10^{-5} rad [38] and it seems possible to produce wave plates with a retardation equal to $\pi/4$ with an accuracy better than 10^{-3} rad. As discussed in Appendix D, it will be necessary to control the plate temperature and the incidence angle in order to keep the retardation at its nominal value but these constraints are not very strong.

In an improved setup, with the defects reduced to a negligible level, the Pancharatnam phase will be an ideal tool to control the phase of an atom interferometer using atom diffraction by laser in the Bragg regime.

(a) The Pancharatnam phase replaces the displacement of a mirror by the rotation of a quarter-wave plate; as it is possible to measure very accurately the rotation of the quarter-wave plate, the variations of the Pancharatnam phase can be controlled with enhanced sensitivity.

(b) As already stated, the Pancharatnam phase being a geometric phase, it is achromatic: Even with imperfect quarter-wave plates, the Pancharatnam phase increases exactly by 2π after a half-turn of QWP2. In order to have the same phase variation for two wavelengths, as needed for a two-species atom interferometer, we need quarter-wave plates with the same retardation at the two wavelengths. Achromatic quarter-wave plates have been produced by combining plates either of materials with different birefringence dispersion [39] or of the same material with different axis orientations [40,41] (for a recent review, see [42]): The usual goal is to produce a retardation as close as possible to $\pi/2$ on a wide spectral range. For a two-species atom interferometer, one needs only to have the same $\pi/2$ retardation for the two wavelengths of interest.

Symmetric interferometers using double diffraction (Bragg or Raman) require one to phase shift the laser standing waves used for the atom beam splitters. The solutions that are currently considered are based on a moving reflection mirror with a PZT. Difficulties associated with these methods (hysteresis, nonlinearities, creep) may limit the performance of the interferometers. The Pancharatnam phase provides a way of controlling the phase shift of an atom interferometer by manipulating the polarization states of the atom beam splitters, which can overcome some limitations provided that high quality optical components are used. Moreover, the geometric character of the Pancharatnam phase allows an identical phase shift simultaneously for two different atomic species, which could find applications the dual atom interferometers developed for a quantum test of the Weak Equivalence Principle, for example.

ACKNOWLEDGMENTS

We thank the laboratory technical and administrative staff for their help. We acknowledge financial support from CNES (Grant No. RS12-SU-0001-034), CNRS INP, ANR (Grant No. ANR-11-BS04-016-01 HIPATI), and Région Midi-Pyrénées.

APPENDIX A: CALCULATION OF THE PANCHARATNAM PHASE

We have chosen to calculate the Pancharatnam phase using the result of Pancharatnam which relates it to the solid angle of the circuit followed by the point representing the polarization on the Poincaré sphere [4,5]. Our choice is based on the tutorial value of this calculation.

Another calculation can be made by using Jones formalism [6] and both calculations give exactly the same result. However, the calculation using Jones formalism involves the multiplication of a series of four 2×2 matrices corresponding to the four traversals of the quarter-wave plates and this explains our choice: Such a product of matrices is very easy to handle thanks to computer programs but the calculation does not give the physical insight that one can get by inspecting the corresponding trajectory on the Poincaré sphere.

The results of Pancharatnam and of Berry prove the geometric nature of the Pancharatnam phase and its independence with the wavelength. This property also appears as a result of the calculation using Jones formalism but without any insight in its origin.

APPENDIX B: PRISMATIC CHARACTER OF THE ROTATING QUARTER-WAVE PLATE QWP2

1. Characterization of the defect

The quarter-wave plates are compound first-order plates, made of two birefringent quartz plates held together by molecular adhesion, the axes of the two plates being crossed. The total thickness is close to 1 mm. The distortion of the wave front of the beam transmitted by these quarter-wave plates is guaranteed to be smaller than $\lambda/10$. Obviously, the plate thickness is not perfectly constant and, in order to characterize this defect, we have measured the variations of this thickness by an interferometric method.

This method is based on the Fabry-Perot dark rings, which can be observed in reflection, even if the two faces are not perfectly parallel but make a small wedge angle α. In a previous publication [43], we have used these dark rings to measure the variation with temperature of the optical path of an uncoated Fabry-Perot. We have used a helium-neon laser emitting at $\lambda = 633$ nm for this measurement: This laser, which emits a few modes extending over a 1-GHz-wide frequency range, is sufficiently monochromatic for the measurement of a 1-mm-thick plate. The antireflection coatings of the quarter-wave plates (reflection coefficient <0.2 % at $\lambda = 671$ nm) reduce the reflected intensity at the laser wavelength $\lambda = 633$ nm and it was necessary to modify our arrangement [43] to work with less reflected light: We replaced the spherical lens by cylindrical lens and the photodiode by a camera. We were thus able to record the ring pattern and to measure the diameters of the three first dark rings with an uncertainty of the order of 1%. Because of the birefringence of the quarter-wave plates, we used linearly polarized light, with a plate axis parallel to the polarization vector.

We do not reproduce here the calculation [43] and simply recall that, from the diameters of the rings, we can deduce the fractional part ε of the quantity $p_0 = 2ne/\lambda$ where n is the index of refraction of the plate (for the chosen polarization) and λ the laser vacuum wavelength. The 1σ uncertainty on $\Delta\varepsilon$ is about 0.02 and we thus get access to the local thickness of the quarter-wave plate at the spot illuminated by the laser with an uncertainty $\Delta e = \lambda\Delta\varepsilon/2n \approx 4$ nm.

By displacing the plate in its plane along two perpendicular directions, covering a rectangle 6×7.5 mm^2 centered on the plate, we get a matrix of ε values from which we can deduce the variation of the plate thickness as can be seen in Fig. 4. We have thus tested the three quarter-wave plates produced by Optique Fichou and we selected for QWP2 the one with the smallest thickness variations. For this plate, the thickness variations are well approximated by assuming that the plate has a wedge angle $\alpha \approx 10$ μrad.

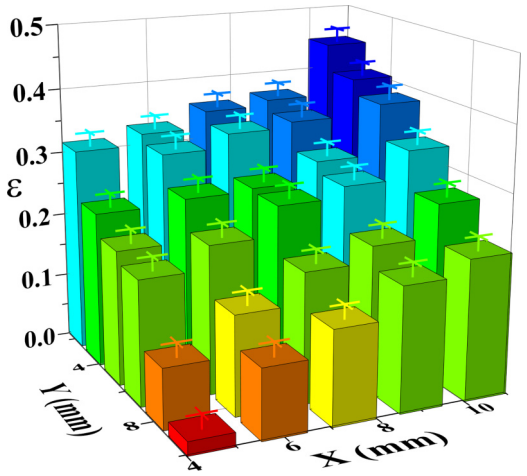

FIG. 4. Fractional part ε of the quantity $p_0 = 2ne/\lambda$ where e is the thickness of the plate QWP2 as a function of the laser spot's position on the plate.

2. Modification of the interference signal

When QWP2 rotates in its plane, the small wedge angle α has two different effects: (i) The quartz thickness traversed by the laser beam axis is modulated by the rotation of the plate if the laser beam axis is not located on the rotation axis, and (ii) the reflected laser beam has a precession motion on a cone.

The first effect induces a periodic variation of the mean optical path (i.e., the optical path measured on the laser beam axis) and this variation modulates the position of the laser standing wave nodes and also the diffraction phase φ_d. The atoms are sensitive to the mean position of these nodes, i.e., to the laser beam axis and this effect is proportional to the distance δr from the laser beam axis to the rotation axis. The resulting variation of φ_d is given by

$$\varphi_{\mathrm{dyn},1} = 2k_L(\bar{n} - 1)\alpha\delta r \cos(\theta - \theta_1). \qquad \text{(B1)}$$

We use the notation $\varphi_{\mathrm{dyn},1}(t)$ because it is a dynamical phase shift as opposed to a geometric phase shift [7]. The factor 2 comes from the fact that QWP2 is crossed twice and $\bar{n}$ is the average of the ordinary and extraodinary refractive indices of crystalline quartz for which $(\bar{n} - 1) \approx 0.547$. The period of this modulation corresponds to a full rotation period of QWP2 and its phase origin θ_1 depends on the prism orientation with respect to the axes of QWP2. For $\delta r = 1$ mm and the measured value of the wedge angle $\alpha \approx 10$ μrad, its amplitude is $\approx$0.1 rad.

The precession of the reflected laser beam due to the second effect has consequences on how accurately the Bragg condition is fulfilled and on the diffraction amplitudes. The half apex angle of the precession cone is $2(\bar{n} - 1)\alpha \approx 9$ μrad.

To describe the consequence of this precession on the interference signal, we should first evaluate the diffraction

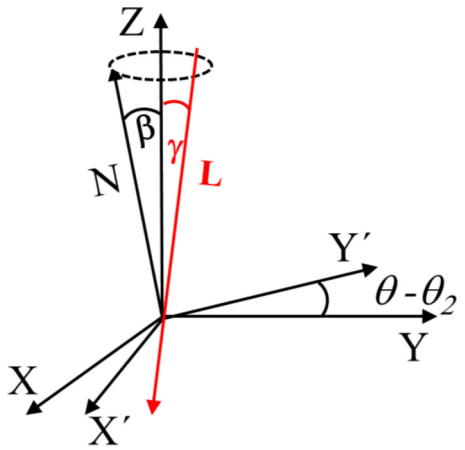

FIG. 5. **L** is the incoming laser beam and **N** the normal of the QWP2 faces. The rotation axe is along **Z** and the rotated frame ($\mathbf{X}'$,$\mathbf{Y}'$,$\mathbf{Z}'$) with $\omega t + \theta$ the rotation angle.

amplitude as a function of the direction of the reflected beam. We should then evaluate the dependence of the signal with this amplitude. We have not tried to make this evaluation because it involves unknown quantities such as the angle between the mean direction of the reflected beam and the QWP's rotation axis or the mismatch of the amplitudes carried by the two interferometer arms. In any case, the resulting effect on the fringe visibility $\mathcal{V}$ should be small because $\mathcal{V}$ varies very slowly around its maximum value which occurs when the two interfering beams have equal amplitudes [28].

APPENDIX C: DEFECTS OF THE ALIGNMENT OF THE OPTICAL COMPONENTS

The rotation axis **R** of QWP2, the normal **N** to its faces, and the laser beam axis **L** are not perfectly parallel. As a result, QWP2's rotation modulates the length of the optical path and we evaluate this effect. In this calculation, it is a good approximation to neglect the prismatic character of QWP2.

We first evaluate the length of the optical path difference Δ due to the introduction of a parallel plate of thickness $\bar{e}$ and refractive index $\bar{n}$ as a function of the incidence angle i and refraction angle $r = \arcsin(\sin(i)/\bar{n})$. For a return path (i.e., a double traversal), we get

$$\Delta = 2\bar{e}\frac{\bar{n} - \cos(i-r)}{\cos(r)} \approx 2\bar{e}\left[(\bar{n}-1) + \frac{i^2(\bar{n}-1)}{2\bar{n}}\right], \quad \text{(C1)}$$

where the approximate form assumes $i \ll 1$.

To estimate the variations of the incidence angle i due to the plate rotation, we must describe the geometry in more details. As shown in Fig. 5, we define a fixed reference frame **X**,**Y**,**Z**, with the rotation axis **R** along **Z** and we choose the **X** axis so that the laser beam axis **L** is in the **X**,**Z** plane, making a small angle γ with **Z**.

$$\mathbf{L} = \mathbf{X}\sin\gamma + \mathbf{Z}\cos\gamma. \quad \text{(C2)}$$

We attach a reference frame $\mathbf{X}'$,$\mathbf{Y}'$,**N** to QWP2 with **N** normal to QWP2. Because of QWP2's rotation around the **Z** axis, **N** makes a constant angle β with the **Z** axis which results in

$$\mathbf{N} = [\mathbf{X}\cos(\theta-\theta_2) + \mathbf{Y}\sin(\theta-\theta_2)]\sin\beta + \mathbf{Z}\cos\beta, \quad \text{(C3)}$$

where θ measures the rotation of the rotatory stages and θ_2 accounts for the initial position of **N**. Equation (C3) describes the precession of **N** around the **Z** axis. Since all the vectors are normalized, we get

$$\begin{aligned}\cos(i) &= \mathbf{N}\cdot\mathbf{L} \\ &= \cos(\beta)\cos(\gamma) + \sin\gamma\sin\beta\cos(\theta-\theta_2) \\ &\approx \left(1-\frac{\beta^2}{2}\right)\left(1-\frac{\gamma^2}{2}\right) - \beta\gamma\cos(\theta-\theta_2). \quad \text{(C4)}\end{aligned}$$

We deduce $i^2 \approx 2[1-\cos(i)]$ from this result and we introduce this value in Eq. (C1). Keeping only the part of Δ which depends on θ, we get the value $\varphi_{\mathrm{dyn},2}$ of the dynamical phase shift due to this alignment defect:

$$\varphi_{\mathrm{dyn},2} \approx 2k_L\bar{e}\frac{\bar{n}-1}{\bar{n}}\beta\gamma\cos(\theta-\theta_2), \quad \text{(C5)}$$

where $\bar{e} \sim 1$ mm is the mean thickness of QWP2. Using a laser beam reflected on QWP2, we have measured the angle $\beta = 10 \pm 1$ mrad. The access to the angle γ is less easy but we estimate that it should not be larger than 5 mrad. For the corresponding maximum value of the product $\beta\gamma = 5\times10^{-5}$ rad^2, the term $\varphi_{\mathrm{dyn},2}$ has an amplitude $\approx$0.3 rad. With a better construction, the two angles β and γ can be reduced by a large factor and this effect should then be reduced to a very low level, below 10^{-3} rad.

APPENDIX D: MODIFICATION OF THE PANCHARATNAM PHASE SHIFT DUE TO DEFECTS OF THE QUARTER-WAVE PLATES

1. The phase shift of the quarter-wave plates

The quarter-wave plates were made by Optique Fichou [31] with the following specifications: first-order quarter-wave plates, phase shift equal to $\pi/2$ with an error smaller than $\pi/150 \approx 21$ mrad. For the design wavelength $\lambda = 671$ nm, the quartz birefringence is equal to $n_e - n_o \approx 9.012\times10^{-3}$ at a temperature 20°C. These quarter-wave plates are compound plates made of two plates of thicknesses e_1 and e_2 close to 500 μm, with a thickness difference $e_1 - e_2 = 18.6 \pm 0.1$ μm chosen to produce a $\pi/2$ retardation.

It is possible to test the phase shift of a quarter-wave plate with a very high sensitivity, below 10^{-3} rad [35–37] or even 10^{-5} rad [38]. We did not perform such an experiment because we did not have the equipment and also because the stated retardation of the available quarter-wave plates was sufficient. However, we calculate the consequences of these defects.

Before presenting this calculation, we first discuss two effects which modify the retardation of a quarter-wave plate, namely the incidence angle i and the temperature dependence of the birefringence.

a. Incidence angle

The retardation ϕ produced by a birefringent plate of thickness e has been calculated as a function of the incidence

TABLE I. Temperature dependence of quartz birefringence $(n_e - n_o)$. We give the reference of the work, the light wavelength λ used for the measurement, and the measured value of the derivative $d(n_e - n_o)/dT$ at a temperature $T = 298$ K. Macé de Lepinay [45] published in 1892 a formula giving the value of $(n_e - n_o)$ as a function of λ and T from which we have extracted the derivative at $\lambda = 671$ nm: This work does not explain if the expansion correction (of the order of 10%) was taken into account. Toyoda and Yabe [48] have measured separately dn_e/dT and dn_o/dT from which we extract $d(n_e - n_o)/dT$ with an uncertainty difficult to evaluate.

Reference	λ (nm)	$d(n_e - n_o)/dT$ (K^{-1})
[31]	671	-1.17×10^{-6}
[45]	671	-1.16×10^{-6}
[46]	633	-1.01×10^{-6}
[47]	1560	-1.02×10^{-6}
[48]	671	-1.3×10^{-6}

angle i, of the angle θ between the plane of incidence and the ordinary axis and the refraction index n_e and n_o. In the limit $i \ll 1$ and using the fact that the quartz birefringence is small, we get

$$\phi \approx k_L e(n_e - n_o)\left\{1 + \frac{i^2}{2n_o n_e}[1 - 2\cos^2(\theta)]\right\}. \quad \text{(D1)}$$

However, as shown by Hale and Day [44], for a compound plate the term dependent on the incidence angle involves the total thickness of the two plates. The maximum effect $\delta\varphi$ is given by

$$\delta\phi(i) \approx k_L(e_1 + e_2)\frac{(n_e - n_o)}{2n_o n_e} i^2. \quad \text{(D2)}$$

If the incidence angle i is always smaller than 15 mrad, the correction $\delta\phi$ of the retardation verifies $|\delta| < 4 \times 10^{-3}$ rad, five times smaller than the specified uncertainty on the retardation $\pi/150 \approx 2 \times 10^{-2}$ rad. As a consequence, we have neglected this variation of the retardation and, as this effect scales as i^2, it can be reduced to a very low value in an improved experiment, with an incidence angle of the order of 1 mrad.

b. Temperature dependence

Quartz birefringence $(n_e - n_o)$ is a function of the temperature T. As shown by Hale and Day [44], a compound plate behaves like a simple plate of thickness $e_1 - e_2$. Table 1 summarizes the information we have collected on the temperature dependence of quartz birefringence. All these results support a value of $d(n_e - n_o)/dT \approx -1.2 \times 10^{-6}$ K^{-1} for $T = 298$ K. As $(n_e - n_o) \approx 9.012 \times 10^{-3}$ at $\lambda = 671$ nm, a temperature variation close to 100 K is needed to modify the retardation ϕ by its specified uncertainty. The temperature of our experiment is stable, near 25°C, and we may safely neglect the effect of the temperature variations on the plate retardation.

2. Modification of the Pancharatnam phase shift due to retardation values different from $\pi/2$

For an ideal setup, the path on the Poincaré sphere is made of two meridians as shown in Fig. 7 and, in this ideal case,

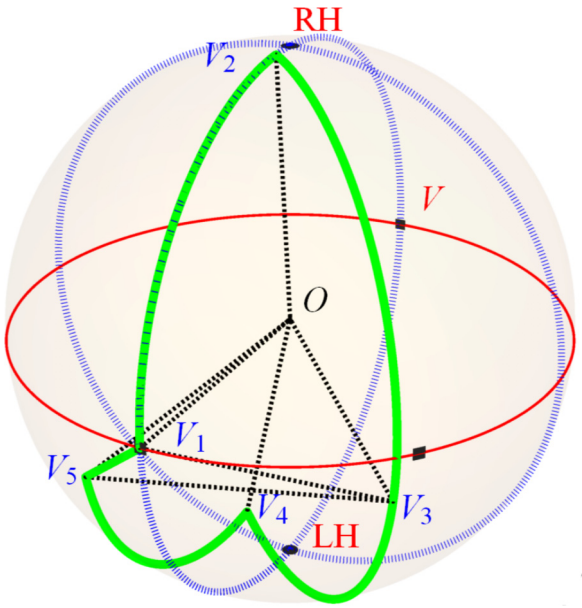

FIG. 6. Trajectory on the Poincaré sphere when the QWP retardations is not perfect. To emphasize the deviation from the perfect trajectory, the QWP's defects for this figure are $\varepsilon_1 = 0.1$ and $\varepsilon_2 = -0.1$.

the calculation of the Pancharatnam phase's solid angle is straightforward. We now consider that the retardation of QWP$_I$ is given by $\pi/2 + \varepsilon_I$ where $\varepsilon_I \ll 1$. The resulting trajectory on the Poincaré sphere is represented in Fig. 6. This trajectory is not closed and we calculate the Pancharatnam phase φ_P by projecting the final state on the initial one. We split the spherical polygon in three spherical triangles $V_1V_2V_3$, $V_3V_4V_5$, and $V_5V_1V_3$. The result is quite voluminous and we give here

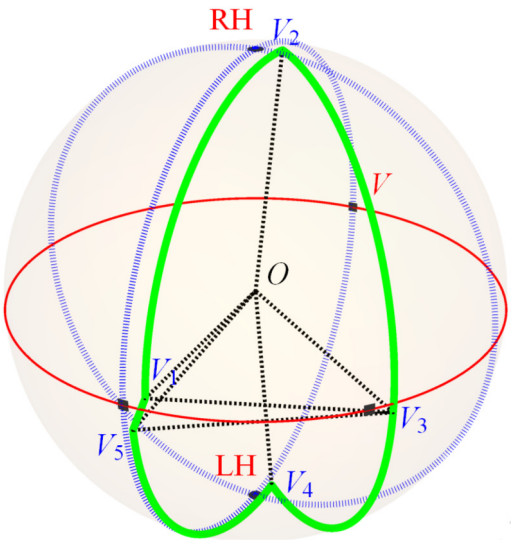

FIG. 7. Trajectory on the Poincaré sphere when the initial polarization is not perfectly linear. For this trajectory, the Stokes parameters for the incident light were $S_1 = 99.5\%$, $S_2 = 8.7\%$, and $S_1 = 4.8\%$ and the QWP were considered perfect. This corresponds to $\epsilon_P = 0.05$ rad and a very small amount of ellipticity.

only its expansion in power series of ε_1 and ε_2:

$$\phi_{P,1}(\theta) \approx 2\theta + 2(\varepsilon_1 + \varepsilon_2)\sin(2\theta) - \varepsilon_1 \sin(4\theta) + \tfrac{3}{4}\left[4\varepsilon_1\varepsilon_2 \sin(2\theta) - \varepsilon_1^2 \sin(4\theta)\right]. \quad \text{(D3)}$$

In addition to the 2θ value of the ideal Pancharatnam phase, we get corrections which are sinusoidal functions of 2θ and 4θ. From the limit on $|\varepsilon_I| < 2 \times 10^{-2}$, we know that the first-order term is smaller than 9×10^{-2} rad while the second-order term is smaller than 2×10^{-3} rad.

a. Modification of the Pancharatnam phase shift by an incorrect incident polarization

Theoretically, the angle between the incident polarization vector and one axis of the quarter-wave plate QWP1 is equal to $\pi/4$ but in our setup, this angle may be slightly different from this ideal value and this modifies the trajectory on the Poincaré (see Fig. 7). If we note $\pi/4 + \epsilon_p$ the value of this angle, we have calculated the Pancharatnam phase as a function of ϵ_p and of the rotation angle θ of QWP2. We get

$$\varphi_{P,2}(\theta) \approx 2\theta + 2\epsilon_p[2\cos(2\theta) - 1 - \cos(4\theta)] - \epsilon_p^2 \sin(4\theta). \quad \text{(D4)}$$

We estimate that $|\epsilon_p| < 30$ mrad and the amplitude of the linear term is smaller than 6×10^{-2} rad while the second-order term is smaller than 10^{-3} rad.

[1] A. D. Cronin, J. Schmiedmayer, and D. E. Pritchard, Rev. Mod. Phys. **81**, 1051 (2009).
[2] Atom interferometry, *Proceedings of The International School of Physics "Enrico Fermi" Course 188*, edited by G. M. Tino and M. A. Kasevich (IOS Press, Amsterdam 2014).
[3] S. Pancharatnam, Proc. Indian Acad. Sci. Sect. A **44**, 247 (1956).
[4] H. Poincaré, Théorie mathématique de la lumière II, G. Carré ed. (Paris, 1892), available on gallica.bnf.fr.
[5] M. Born and E. Wolf, *Principles of Optics*, 4th ed. (Pergamon Press, Oxford, 1970).
[6] R. Clark Jones, J. Opt. Soc. Am. **31**, 488 (1941); **31**, 493 (1941); **31**, 500 (1941).
[7] M. V. Berry, Proc. R. Soc. Lond. A **392**, 45 (1984).
[8] M. V. Berry, J. Mod. Opt. **34**, 1401 (1987).
[9] R. Bhandari, Phys. Rep. **281**, 1 (1997).
[10] N. Baba, N. Murakami, and T. Ishigaki, Opt. Lett. **26**, 1167 (2001).
[11] C. J. Bordé, in *Atom Interferometry*, edited by P. R. Berman (Academic Press, San Diego, 1997), p. 257.
[12] S. Fray, C. A. Diez, T. W. Hänsch, and M. Weitz, Phys. Rev. Lett. **93**, 240404 (2004).
[13] R. Geiger *et al.*, Nat. Commun. **2**, 474 (2011).
[14] D. Schlippert, J. Hartwig, H. Albers, L. L. Richardson, C. Schubert, A. Roura, W. P. Schleich, W. Ertmer, and E. M. Rasel, Phys. Rev. Lett. **112**, 203002 (2014).
[15] B. Barrett, L. Antoni-Micollier, L. Chichet, B. Battelier, P. A. Gominet, A. Bertoldi, P. Bouyer, and A. Landragin, New J. Phys. **17**, 085010 (2015).
[16] J. Hartwig, S. Abend, C. Schubert, D. Schlippert, H. Ahlers, K. Posso-Trujillo, N. Gaaloul, W. Ertmer, and E. M. Rasel, New J. Phys. **17**, 035011 (2015).
[17] J. Williams, S.-W. Chiow, N. Yu, and H. Müller, New J. Phys. **18**, 025018 (2016).
[18] G. T. Foster, J. B. Fixler, J. M. McGuirk, and M. A. Kasevich, Opt. Lett. **27**, 951 (2002).
[19] G. Rosi, F. Sorrentino, L. Cacciapuoti, M. Prevedelli, and G. M. Tino, Nature **510**, 518 (2014).
[20] M. J. Collett and G. J. Tee, J. Opt. Soc. Am. A **31**, 2573 (2014).
[21] L. R. Watkins and M. J. Collett, Appl. Opt. **53**, 7697 (2014).
[22] M. J. Collett and L. R. Watkins, J. Opt. Soc. Am. A **32**, 491 (2015).
[23] C. Robens, J. Zopes, W. Alt, S. Brakhane, D. Meschede, and A. Alberti, Phys. Rev. Lett. **118**, 065302 (2017).
[24] T. H. Chyba, L. J. Wang, L. Mandel, and R. Simon, Opt. Lett. **13**, 562 (1988).
[25] R. Simon, H. J. Kimble, and E. C. G. Sudarshan, Phys. Rev. Lett. **61**, 19 (1988).
[26] R. Bhandari and J. Samuel, Phys. Rev. Lett. **60**, 1211 (1988).
[27] R. Bhandari, Phys. Lett. A **133**, 1 (1988).
[28] A. Miffre, M. Jacquey, M. Büchner, G. Trénec, and J. Vigué, Eur. Phys. J. D **33**, 99 (2005).
[29] A. Miffre, PhD. thesis, Université P. Sabatier (2005), available on http://tel.archives-ouvertes.fr/.
[30] S. Lepoutre, V. P. A. Lonij, H. Jelassi, G. Trénec, M. Büchner, A. D. Cronin, and J. Vigué, Eur. Phys. J. D **62**, 309 (2011).
[31] Optique Fichou website http://optique-fichou.com/ and private communication.
[32] A. Miffre, M. Jacquey, M. Büchner, G. Trénec, and J. Vigué, Appl. Phys. B: Lasers Opt. **84**, 617 (2006).
[33] M. Jacquey, A. Miffre, M. Büchner, G. Trénec, and J. Vigué, Europhys. Lett. **77**, 20007 (2007).
[34] J. Gillot, A. Gauguet, M. Büchner, and J. Vigué, Eur. Phys. J. D **67**, 263 (2013).
[35] L. Yao, Z. Zhiyao, and W. Runwen, Opt. Lett. **13**, 553 (1988).
[36] S. Nakadate, Appl. Opt. **29**, 242 (1990).
[37] W. Liu, M. Liu, and S. Zhang, Appl. Opt. **47**, 5562 (2008).
[38] S. M. Wilson, V. Vats, and P. H. Vaccaro, J. Opt. Soc. Am. B **24**, 2500 (2007).
[39] C. D. West and A. S. Maicas, JOSA **39**, 791 (1949).
[40] S. Pancharatnam, Proc. Indian Acad. Sci. Sect. A **41**, 137 (1955).
[41] C. M. McIntyre and S. E. Harris, JOSA **58**, 1575 (1968).
[42] J. M. Herrera-Fernandez, J. L. Vilas, L. M. Sanchez-Brea, and E. Bernabeu, Appl. Opt. **54**, 9758 (2015).
[43] P.-E. Dupouy, M. Büchner, P. Paquier, G. Trńec, and J. Vigué, Appl. Opt. **49**, 678 (2010).
[44] P. D. Hale and G. W. Day, Appl. Opt. **27**, 5146 (1988).
[45] J. Macé de Lépinay, J. Phys. Theor. Appl. **1**, 23 (1892).
[46] S. De Nicola, G. Carbonara, A. Finizio, and G. Pierattini, Appl. Phys. B **58**, 133 (1994).
[47] V. Ivanov, M. Levichev, Y. Nozdrin, and M. Novikov, Appl. Opt. **54**, 9911 (2015).
[48] T. Toyoda and M. Yabe, J. Phys. D: Appl. Phys. **16**, L97 (1983).